Proceedings of the ASME 2009 Conference on Smart Materials, Adaptive Structures and Intelligent Systems
SMASIS2009
September 21-23, 2009, Oxnard, California, USA

SMASIS2009-1263

A STATE-SPACE TEMPORAL FINITE ELEMENT APPROACH FOR STABILITY INVESTIGATIONS OF DELAY EQUATIONS

Firas A. Khasawneh*
Brian P. Mann
Department of Mechanical Engineering
and Materials Science
Duke University
Durham, North Carolina 27708
Email: firas.khasawneh@duke.edu
brian.mann@duke.edu

Bhavin Patel
Wayne Engineering
701 Performance Drive
Cedar Falls, IA 50613-6952
Email: bpatel@wayneusa.com

ABSTRACT
This paper describes a new approach to examine the stability of delay differential equations that builds upon prior work using temporal finite element analysis. In contrast to previous analyses, which could only be applied to second order delay differential equations, the present manuscript develops an approach which can be applied to a broader class of systems - systems that may be written in the form of a state space model. A primary outcome from this work is a generalized framework to investigate the asymptotic stability of autonomous delay differential equations with a single time delay. Furthermore, this approach is shown to be applicable to time-periodic delay differential equations and equations that are piecewise continuous.

INTRODUCTION
It has been known for quite some time that several systems can be described by models that include past effects. These systems, where the rate of change in a state is determined by both the past and the present states, are described by delay differential equations (DDE). Examples from recent literature include applications in robotics, biology, human response time, economics and manufacturing processes [1–4]. The qualitative study of these types of dynamical systems often involves a stability analysis, which is presented in the form of stability charts that show the system stability over a range of parameters [5–9]. A primary complexity for delay systems lies in the fact that they are infinite dimensional. In particular, it is well-know that introducing a time delay into a dynamical system causes the phase space to grow from a finite dimension to an infinite dimension [10, 11].

A linear autonomous DDE with a single delay can be described by

$$\dot{\mathbf{y}}(t) = \mathbf{A}\mathbf{y}(t) + \mathbf{B}\mathbf{y}(t-\tau)\,, \tag{1}$$

where $\mathbf{A}$ and $\mathbf{B}$ are square matrices and the delay $\tau > 0$. The characteristic equation for the above system, which is obtained by assuming an exponential solution, becomes

$$|\lambda\mathbf{I} - \mathbf{A} - \mathbf{B}e^{-\lambda\tau}| = 0\,. \tag{2}$$

As compared to the characteristic equation for an autonomous ordinary differential equation (ODE), Eq. (2) has an infinite number of roots. The necessary and sufficient condition for asymptotic stability is that all the characteristic roots must have negative real parts [11]. A discrete solution form for Eq. (1) that maps the states of the system over a single delay period can be written

*Corresponding author

Copyright © 2009 by ASME

as a discrete map of the form

$$\mathbf{y}_n = \mathbf{M}\,\mathbf{y}_{n-1}\,, \tag{3}$$

where $\mathbf{y}$ is the state variable during either the current or previous delay period - as denoted by the subscripts n and $n-1$. Here, the condition for asymptotically stability requires that the infinite number of characteristic multipliers, or eigenvalues of $\mathbf{M}$, must be in a modulus of less than one.

Another general case to consider is the stability of a time periodic system with a single delay. The general expression for this type of system is

$$\dot{\mathbf{y}}(t) = \mathbf{A}(t)\mathbf{y}(t) + \mathbf{B}(t)\mathbf{y}(t-\tau)\,, \tag{4}$$

where T is the period of $\mathbf{A}(t)$ and $\mathbf{B}(t)$ which stipulates the following condition $\mathbf{A}(t+T) = \mathbf{A}(t)$ and $\mathbf{B}(t+T) = \mathbf{B}(t)$. Analogous to the time-periodic ODE case, the solution can be written in the form $\mathbf{y} = \mathbf{p}(t)e^{\lambda t}$, where $\mathbf{p}(t) = \mathbf{p}(t+T)$. However, a primary difference exist between the dynamic map equation of a time periodic ODE and a time periodic DDE, which can also be written as Eq. (3), since the monodromy operator, $\mathbf{M}$, for the DDE becomes infinite dimensional. Although the time periodic system will have a finite dimensional Floquet transition matrix, the delay system will have an infinite dimensional monodromy operator [12]. Also, in contrast to the classical time periodic case, the time delayed system will have an infinite number of characteristic multipliers. The resulting criteria for asymptotic stability requires the infinite number of characteristic multipliers to have a modulus of less than one; this criteria is analogous to requiring the infinite number of characteristic exponents to be negative and real for a continuous system.

The fact that the mondromy operator is infinite dimensional prohibits a closed-formed solution. In spite of this, one can approach this problem from a practical standpoint - by constructing a finite dimensional monodromy operator that closely approximates the stability characteristics of the infinite dimensional monodromy operator. This is the underlying approach that is followed throughout this manuscript and in numerous other previous works using discretization methods to examine delay equations [1, 13, 14].

A number of prior works have used time finite elements to predict the dynamic behavior of a system (e.g. see references [15–17]). However, temporal finite element analysis was first used to determine the stability of delay equations in reference [7]. The authors examined a second order delay equation that was piecewise continuous with constant coefficients. Following a similar methodology, the approach was adapted to examine second order delay equations with time-periodic coefficients and piecewise continuity in references [1, 13, 18]. Although these prior analyses did provide a computationally efficient approach, the presented methodology was limited to governing equations that could be written in the form of a second order DDE. A distinguishing feature of the present approach is the presentation of a temporal finite element approach that can be used to determine the stability characteristics of DDEs that are in the form of a state space model [19]. Essentially, this work extends the usefulness of the temporal finite element method to a broader class of systems with time delays. Thus, this manuscript investigates both systems that could not be examined by the aforementioned approach and examples that show agreement with the prior work.

The content of this paper is organized as follows. The next section describes the formulation of a temporal finite element analysis approach for autonomous delay equations. The stability of a single state system is examined prior to presenting a more general analysis that can be applied to autonomous as well as non-autonomous DDEs with an arbitrary number of states. The stability analysis of a third order autonoumou DDE, which could not be handled using the prior TFEA approach, is then described. The subtle differences required to handle systems that are time periodic are demonstrated through a stability analysis of an interrupted turning process. The interrupted turning example also highlights a particularly important feature of this method - the ability to handle both continuous and piecewise continuous DDEs.

AUTONOMOUS DELAY SYSTEM

A distinguishing feature of autonomous systems is that time does not explicitly appear in the governing equations. Some application areas where autonomous DDEs arise are in robotics, biology, and control using sensor fusion. In an effort to improve the clarity of this section, we first consider the analysis of a scalar DDE before describing the generalized approach. Thus, the stability analysis of the scalar DDE is followed by an analysis of the general case of a DDE with multiple states written in matrix-vector form.

Scalar Autonomous DDE

Time Finite Element Analysis (TFEA) is a discretization approach that divides the time interval of interest into a finite number of temporal elements. This approach allows the original DDE to be transformed into the form of a discrete map. The asymptotic stability of the system is then analyzed from the characteristic multipliers or eigenvalues of the map. While previous works for the TFEA method have solely focused on second order DDEs [1, 7, 13, 18], the goal here is to present a new approach that is also applicable to first order DDEs with a single time delay. For instance, we consider the following time delay system, originally examined by Hayes [20], that has a single state vari-

Copyright © 2009 by ASME

able

$$\dot{y}(t) = \alpha\, y(t) + \beta\, y(t-\tau)\,, \tag{5}$$

where α and β are scalar control parameters and $\tau = 1$ is the time delay. Since the Eq (5) does not have a closed form solution, the first step in the analysis is to consider an approximate solution for the j^{th} element of the n^{th} period as a linear combination of polynomials or trial functions. The assumed solution for the state and the delayed state are

$$y_j(t) = \sum_{i=1}^{3} a_{ji}^{n}\phi_i(\sigma)\ , \tag{6a}$$

$$y_j(t-\tau) = \sum_{i=1}^{3} a_{ji}^{n-1}\phi_i(\sigma)\,, \tag{6b}$$

where a superscript is used to denote the n^{th} and $n-1$ period for the current and delayed state variable, respectively. Each trial function, $\phi_i(\sigma)$, is written as a function of the local time, σ, within the j^{th} element and the local time is allowed to vary from zero to the time for each element, t_j. The introduction of a local time variable is beneficial because it allows a set of trial functions to remain orthogonal on an interval $0 \le \sigma \le t_j$ once they have been normalized. To further clarify the local time concept, assume that E elements are used in the analysis and that the time for each element is taken to be uniform, then the time interval for a single element is $t_j = \tau/E$ and the local time would vary from zero to t_j. Furthermore, a set of trial functions orthogonal on the interval from zero to one can made orthogonal over any $0 \le \sigma \le t_j$ interval by simply replacing the original independent variable for the polynomials with σ/t_j. The polynomials used for this analysis are

$$\phi_1(\sigma) = 1 - 23\left(\frac{\sigma}{t_j}\right)^2 + 66\left(\frac{\sigma}{t_j}\right)^3 - 68\left(\frac{\sigma}{t_j}\right)^4 + 24\left(\frac{\sigma}{t_j}\right)^5 , \tag{7a}$$

$$\phi_2(\sigma) = 16\left(\frac{\sigma}{t_j}\right)^2 - 32\left(\frac{\sigma}{t_j}\right)^3 + 16\left(\frac{\sigma}{t_j}\right)^4 , \tag{7b}$$

$$\phi_3(\sigma) = 7\left(\frac{\sigma}{t_j}\right)^2 - 34\left(\frac{\sigma}{t_j}\right)^3 + 52\left(\frac{\sigma}{t_j}\right)^4 - 24\left(\frac{\sigma}{t_j}\right)^5 . \tag{7c}$$

The above trial functions are orthogonal on the interval of $0 \le \sigma \le t_j$ and they are obtained through interpolation. The interpolated trial functions are constructed such that the coefficients of the assumed solution directly represents the state variable at the beginning $\sigma = 0$, middle $\sigma = t_j/2$, and end $\sigma = t_j$ of each temporal element. The graph of Fig. 1 is provided to illustrate the important fact that the coefficients of the assumed solution take on the values of the state variables at specific instances in time. Thus, these functions satisfy the natural and essential boundary conditions (i.e. the states at the end of one element match those at the beginning of the following element).

Substituting Eq. (6a) and Eq. (6b) into Eq. (5) results in the following

$$\sum_{i=1}^{3}\left(a_{ji}^{n}\dot{\phi_i}(\sigma) - \alpha a_{ji}^{n}\phi_i(\sigma) - \beta a_{ji}^{n-1}\phi_i(\sigma)\right) = \text{error}\,, \tag{8}$$

which shows a non-zero error associated with the approximate solutions of Eq. (6a) and Eq. (6b). In order to minimize this error, the assumed solution is weighted by multiplying by a set of test functions, or so called weighting functions, and the integral of the weighted error is set to zero. This is called the method of weighted residuals and requires that the weighting functions be linearly independent [21]. The weighting functions used for the presented analysis were shifted Legendre polynomials. These polynomials were used because they satisfy the required condition of linear independence. Here, we have chosen to only use the first two shifted Legendre polynomials $\psi_1(\sigma) = 1$ and $\psi_2(\sigma) = 2(\sigma/t_j) - 1$ to keep the matrices square. The weighted error expression becomes

$$\int_0^{t_j}\left[\sum_{i=1}^{3}\left(a_{ji}^{n}\dot{\phi_i}(\sigma) - \alpha a_{ji}^{n}\phi_i(\sigma) - \beta a_{ji}^{n-1}\phi_i(\sigma)\right)\right]\psi_p(\sigma)d\sigma = 0\,. \tag{9}$$

After applying each weighting function, a global matrix equation can be obtained by combining the resulting equations for each element. To provide a representative expression, we assume two elements are sufficient and write the global matrix of Eq. (10). This equation relates the states of the system in the current period to the states of the system in the previous period,

$$\begin{bmatrix} 1 & 0 & 0 & 0 & 0 \\ N_{11}^1 & N_{12}^1 & N_{13}^1 & 0 & 0 \\ N_{21}^1 & N_{22}^1 & N_{23}^1 & 0 & 0 \\ 0 & 0 & N_{11}^2 & N_{12}^2 & N_{13}^2 \\ 0 & 0 & N_{21}^2 & N_{22}^2 & N_{23}^2 \end{bmatrix} \begin{bmatrix} a_{11} \\ a_{12} \\ a_{21} \\ a_{22} \\ a_{23} \end{bmatrix}^n = \begin{bmatrix} 0 & 0 & 0 & 0 & 1 \\ P_{11}^1 & P_{12}^1 & P_{13}^1 & 0 & 0 \\ P_{21}^1 & P_{22}^1 & P_{23}^1 & 0 & 0 \\ 0 & 0 & P_{11}^2 & P_{12}^2 & P_{13}^2 \\ 0 & 0 & P_{21}^2 & P_{22}^2 & P_{23}^2 \end{bmatrix} \begin{bmatrix} a_{11} \\ a_{12} \\ a_{21} \\ a_{22} \\ a_{23} \end{bmatrix}^{n-1} . \tag{10}$$

The terms inside the matrices of Eq. (10) are the following scalar

Copyright © 2009 by ASME

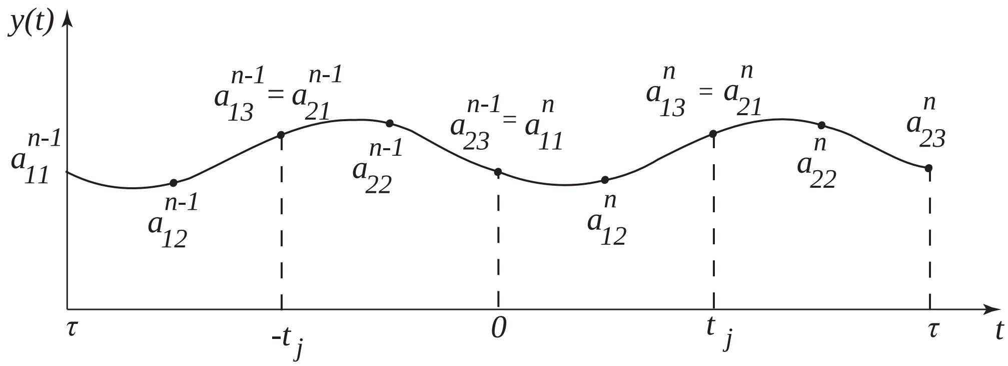

Figure 1. Time line for the state variable, y, over a time interval of 2τ. Dots denote the locations where the coefficients of the assumed solution are equivalent to the state variable. The beginning and end of each temporal element is marked with dotted lines.

terms

$$N^j_{pi} = \int_0^{t_j} \left(\dot{\phi}_i(\sigma) - \alpha\phi_i(\sigma)\right)\psi_p(\sigma)\, d\sigma\,, \tag{11a}$$

$$P^j_{pi} = \int_0^{t_j} \beta\phi_i(\sigma)\psi_p(\sigma)\, d\sigma\,. \tag{11b}$$

If the time interval for each element is identical, the superscript in these expressions can be dropped for autonomous systems since the expressions for each element would be identical. However, the use of non-uniform time elements or the examination of non-autonomous will typically require the superscript notation.

Equation (10) describes a discrete time system or a dynamic map that can be written in a more compact form $\mathbf{G}\mathbf{a}_n = \mathbf{H}\mathbf{a}_{n-1}$ where the elements of the $\mathbf{G}$ matrix are defined by each N^j_{pi} term of Eq. (11a). Correspondingly, the elements of the $\mathbf{H}$ matrix are defined by the P^j_{pi} terms from Eq. (11b). Multiplying the dynamic map expression by $\mathbf{G}^{-1}$ results in $\mathbf{a}_n = \mathbf{Q}\mathbf{a}_{n-1}$ where $\mathbf{Q}$= $\mathbf{G}^{-1}\mathbf{H}$. Applying the conditions of the chosen trial functions to the beginning, midpoint, and end conditions allows us to replace $\mathbf{a}_n$ and $\mathbf{a}_{n-1}$ with $\mathbf{y}_n$ and $\mathbf{y}_{n-1}$, respectively. Here, $\mathbf{y}_n$ is the vector that represents the state variable at the beginning, middle, end of each temporal finite element. Thus, the the final expression becomes

$$\mathbf{y}_n = \mathbf{Q}\mathbf{y}_{n-1}\,, \tag{12}$$

which represents a map of the state variable over a single delay period (i.e. the $\mathbf{Q}$ matrix relates the state variable at time instances that correspond to the beginning, middle, and end of each element to the state variable one period into the future).

The eigenvalues of the monodromy operator $\mathbf{Q}$ are called characteristic multipliers. The criteria for asymptotic stability requires that the magnitudes of the characteristic multipliers must be in the modulus of less than one for a given combination of the control parameters, see Fig. 3.

Figure 2(a) shows the boundaries between stable and unstable regions as a function of the control parameters α and β. The characteristic multipliers trajectories of Fig. 2(b) show how changes in a single control parameter can cause the characteristic multipliers to exit the unit circle in the complex plane.

GENERALIZATION FOR LINEAR DDES

While the scalar case was provided as an introductory example, it is more likely that the practitioner will encounter the case of a first order DDE with multiple states. Thus, the goal of this section is to describe the generalized analysis and its application to some illustrative problems.

The general analysis assumes a state space system in the form of Eq. (1). The expressions for state and the delayed state variables are now written as vectors

$$\mathbf{y}_j(t) = \sum_{i=1}^{3} \mathbf{a}^{\,n}_{ji}\phi_i(\sigma)\ , \tag{13a}$$

$$\mathbf{y}_j(t-\tau) = \sum_{i=1}^{3} \mathbf{a}^{\,n-1}_{ji}\phi_i(\sigma)\,. \tag{13b}$$

during the j^{th} element. After substituting the assumed solution forms into Eq. (1) and applying the method of weighted residuals, a global matrix can be obtained that relates the states of the

Copyright © 2009 by ASME

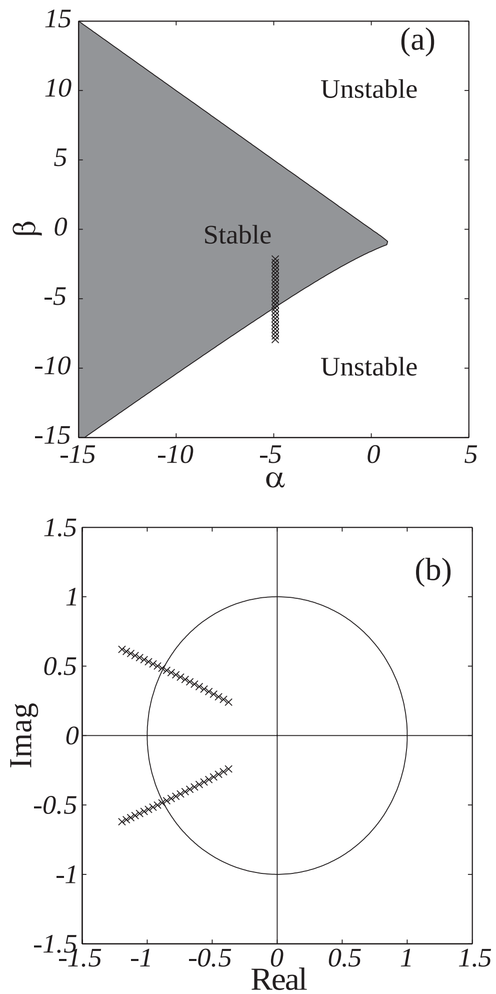

Figure 2. A converged stability chart (graph (a)) for Eq. (5) is obtained when using a single temporal element and $\tau = 1$. Stable domains are shaded and unstable parameter domains are unshaded. Graph (b) shows the CM trajectories in complex plane for $\alpha = 4.9$ and a range of values for β.

system in the current period to those in the previous period,

$$\begin{bmatrix} \mathbf{I} & 0 & 0 & 0 & 0 \\ \mathbf{N}_{11}^1 & \mathbf{N}_{12}^1 & \mathbf{N}_{13}^1 & 0 & 0 \\ \mathbf{N}_{21}^1 & \mathbf{N}_{22}^1 & \mathbf{N}_{23}^1 & 0 & 0 \\ 0 & 0 & \mathbf{N}_{11}^2 & \mathbf{N}_{12}^2 & \mathbf{N}_{13}^2 \\ 0 & 0 & \mathbf{N}_{21}^2 & \mathbf{N}_{22}^2 & \mathbf{N}_{23}^2 \end{bmatrix} \begin{bmatrix} \mathbf{a}_{11} \\ \mathbf{a}_{12} \\ \mathbf{a}_{21} \\ \mathbf{a}_{22} \\ \mathbf{a}_{23} \end{bmatrix}^n = \begin{bmatrix} 0 & 0 & 0 & 0 & \mathbf{\Phi} \\ \mathbf{P}_{11}^1 & \mathbf{P}_{12}^1 & \mathbf{P}_{13}^1 & 0 & 0 \\ \mathbf{P}_{21}^1 & \mathbf{P}_{22}^1 & \mathbf{P}_{23}^1 & 0 & 0 \\ 0 & 0 & \mathbf{P}_{11}^2 & \mathbf{P}_{12}^2 & \mathbf{P}_{13}^2 \\ 0 & 0 & \mathbf{P}_{21}^2 & \mathbf{P}_{22}^2 & \mathbf{P}_{23}^2 \end{bmatrix} \begin{bmatrix} \mathbf{a}_{11} \\ \mathbf{a}_{12} \\ \mathbf{a}_{21} \\ \mathbf{a}_{22} \\ \mathbf{a}_{23} \end{bmatrix}^{n-1}, \quad (14)$$

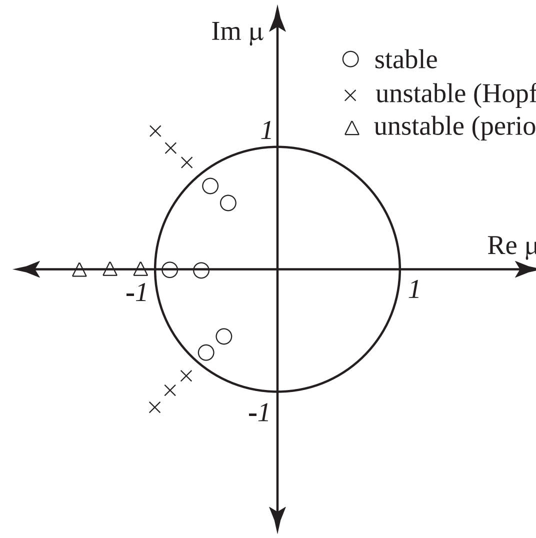

Figure 3. The stability criteria dictates that all the eigenvalues, μ, of the monodromy operator $\mathbf{Q}$, should lie within the unit circle in the complex plane. Moreover, the manner in which the eigenvalues depart the unit circle produces different bifurcation behavior. For example, an eigenvalue leaving the unit circle through -1 results in a period doubling bifurcation whereas two complex conjugate eigenvalues departing the unit circle results in secondary Hopf bifurcation.

where $\mathbf{I}$ is an identity matrix and the terms $\mathbf{N}_{pi}^j$ and $\mathbf{P}_{pi}^j$ now become the following square matrices

$$\mathbf{N}_{pi}^j = \int_0^{t_j} \Big(\mathbf{I}\dot{\phi}_i(\sigma) - \mathbf{A}\phi_i(\sigma)\Big)\psi_p(\sigma)\, d\sigma\,, \quad (15a)$$

$$\mathbf{P}_{pi}^j = \int_0^{t_j} \mathbf{B}\phi_i(\sigma)\psi_p(\sigma)\, d\sigma\,, \quad (15b)$$

Here, we note the $\mathbf{\Phi}$ matrix is the identity matrix when the delay terms are always present. However, $\mathbf{\Phi}$ may not always be the identity matrix for systems that are piecewise continuous as we will show later. The dimensions of the matrices $\mathbf{I}$, $\mathbf{\Phi}$, $\mathbf{N}_{pi}^j$ and $\mathbf{P}_{pi}^j$ are the same as the dimensions of $\mathbf{A}$ and $\mathbf{B}$.

The presented approach can also be applied to non-autonomous DDEs on the form of Eq. (4) as long as a few subtle changes are implemented. In this case, the time dependence of the matrices $\mathbf{A}(t)$ and $\mathbf{B}(t)$ requires the substitution $t = \sigma + (j-1)t_j$ so that the time periodic terms take on the correct values over the entire period. This substitution changes

Copyright © 2009 by ASME

the expressions for $\mathbf{N}$ and $\mathbf{P}$ according to

$$\mathbf{N}_{pi}^{j} = \int_0^{t_j} \Big(\mathbf{I}\dot{\phi_i}(\sigma) - \mathbf{A}\big(\sigma+(j-1)t_j\big)\,\phi_i(\sigma)\Big)\psi_p(\sigma)\,d\sigma\,, \tag{16a}$$

$$\mathbf{P}_{pi}^{j} = \int_0^{t_j} \mathbf{B}\big(\sigma+(j-1)t_j\big)\phi_i(\sigma)\psi_p(\sigma)\,d\sigma\,, \tag{16b}$$

and $\mathbf{\Phi}$ is taken to be the identity matrix. Here, we point out that the superscript, j, may not be dropped in the above expressions since the time-periodic terms of $\mathbf{A}\big(\sigma+(j-1)t_j\big)$ will assume different values within each element. Using the above expressions, a dynamic map for the non-autonomous case can be constructed similar to Eq. (14).

The dynamic map of Eq. (14) is then written in a more compact form, $\mathbf{G}\mathbf{a}_n = \mathbf{H}\mathbf{a}_{n-1}$ where the elements of the $\mathbf{G}$ matrix are defined by each $\mathbf{N}_{pi}^{j}$ term of Eq. (15a). Correspondingly, the elements of the $\mathbf{H}$ matrix are defined by the $\mathbf{P}_{pi}^{j}$ terms from Eq. (15b). Evaluating the chosen trial functions at the beginning, midpoint, and end of each element allows the coefficients of the assumed solution, $\mathbf{a}_n$ and $\mathbf{a}_{n-1}$, to be replaced with $\mathbf{y}_n$ and $\mathbf{y}_{n-1}$, respectively. An eigenvalue problem is then formed by multiplying the dynamic map expression by $\mathbf{G}^{-1}$ and taking the eigenvalues of matrix $\mathbf{Q}$= $\mathbf{G}^{-1}\mathbf{H}$. Alternatively, one may wish to avoid the complication of inverting $\mathbf{G}$, as in the case that $\mathbf{G}$ is close to singular, and would instead prefer to solve for the μ values (the characteristic multipliers) that solve the characteristic equation that is obtained by setting the determinant of $\mathbf{H} - \mu\mathbf{G}$ equal to zero.

Example Autonomous Third Order DDE

Determining the stability of a third order delay equation would not have been possible with the prior TFEA analyses [1, 7, 13, 18]. Thus, we consider the following third order delay equation

$$\frac{d^3x}{dt^3} + \alpha\dot{x} + \beta x(t-\tau) = 0\,, \tag{17}$$

with a delay of $\tau = 1$ and control parameters α and β. The state space form of Eq. (17) is

$$\begin{bmatrix}\dot{y_1}\\ \dot{y_2}\\ \dot{y_3}\end{bmatrix} = \begin{bmatrix}0 & 1 & 0\\ 0 & 0 & 1\\ 0 & -\alpha & 0\end{bmatrix}\begin{bmatrix}y_1\\ y_2\\ y_3\end{bmatrix} + \begin{bmatrix}0 & 0 & 0\\ 0 & 0 & 0\\ -\beta & 0 & 0\end{bmatrix}\begin{bmatrix}y_1(t-\tau)\\ y_2(t-\tau)\\ y_3(t-\tau)\end{bmatrix}\,, \tag{18}$$

where $y_1 = x$, $y_2 = \dot{x}$, and $y_3 = \ddot{x}$. The $\mathbf{A}$ and $\mathbf{B}$ matrices of Eq. (1) become

$$\mathbf{A} = \begin{bmatrix}0 & 1 & 0\\ 0 & 0 & 1\\ 0 & -\alpha & 0\end{bmatrix} \quad \text{and} \quad \mathbf{B} = \begin{bmatrix}0 & 1 & 0\\ 0 & 0 & 1\\ 0 & -\alpha & 0\end{bmatrix}\,. \tag{19}$$

Determining the stability requires the dynamic map of Eq. (14) to be populated with the integral expressions of Eq. (15a) and Eq. (15b) where the $\mathbf{A}$ and $\mathbf{B}$ matrices of Eq. (19) have been used. Since the system of interest is continuous, a 3×3 identity matrix is used for $\mathbf{\Phi}$. An example stability chart was constructed for this system and is shown in Fig. 4. As noted by reference [10], the stability chart for this system becomes a series of geometric shapes with stability borders defined by the intersection of lines.

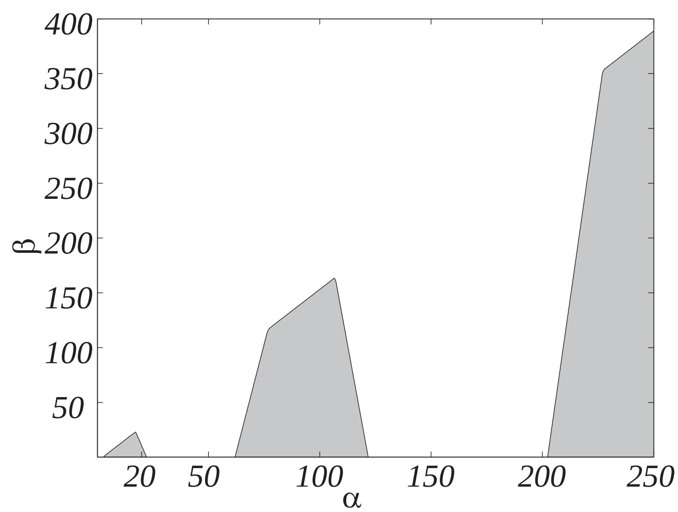

Figure 4. Stability chart for the autonomous system of Eq. (17) obtained using $\tau = 1$ and eight elements. Stable regions are shaded and unstable regions are left blank.

Example Piecewise Continuous and Time Periodic DDE-Interrupted Turning

Interrupted turning is a piece-wise continuous system where the tool is not always cutting but enters and exits the cut, see Fig 5. When the tool is in the cut, a force proportional to the uncut chip area acts on the tool; however, when the tool exits the cut, the system will undergo free vibration. As an example, an interrupted turning process where the workpiece is rigid and

Copyright © 2009 by ASME

the tool is compliant in only one direction will be considered. The variational equation of motion for this system can be written as [23]

$$\ddot{\xi}(t)+2\zeta\omega_{\mathrm{n}}\,\dot{\xi}(t)+\omega_{\mathrm{n}}^{2}\,\xi(t)=-u(t)\,\frac{k_1 b}{m}(\xi(t)-\xi(t-\tau)) \quad (20)$$

where ζ is damping, ω_{n} is the natural frequency, m is the mass, b is the depth of cut, k_1 is a cutting parameter, and $u(t)$ is a switching function: its value is 1 when the tool is cutting, and 0 when the tool exits the cut.

A set of dimensionless parameters for time, spindle speed, time delay and depth of cut is defined as [24]

$$\tilde{t}=\omega_{\mathrm{n}}t,\;\; \tilde{\Omega}=\frac{\Omega}{\omega_{\mathrm{n}}},\;\; \tilde{\tau}=\omega_{\mathrm{n}}\tau,\;\; \tilde{b}=\frac{bk_1}{m\omega_{\mathrm{n}}^{2}}. \quad (21)$$

These substitutions result in the dimensionless characteristic frequency $\tilde{\omega}_{\mathrm{n}}=1$. The non-dimensionalized version of Eq. (20) then reads

$$\ddot{\xi}(\tilde{t})+2\zeta\,\dot{\xi}(\tilde{t})+\xi(\tilde{t})=-u(t)\,\tilde{b}(\xi(\tilde{t})-\xi(\tilde{t}-\tilde{\tau})). \quad (22)$$

Equation (22) can be written in state-space form as

$$\begin{bmatrix}\dot{x}_1\\ \dot{x}_2\end{bmatrix}=\begin{bmatrix}0 & 1\\ -(u(t)\,\tilde{b}+1) & -2\zeta\end{bmatrix}\begin{bmatrix}x_1\\ x_2\end{bmatrix}+\begin{bmatrix}0 & 0\\ u(t)\,\tilde{b} & 0\end{bmatrix}\begin{bmatrix}x_1(t-\tau)\\ x_2(t-\tau)\end{bmatrix}, \quad (23)$$

where the tilde was dropped from t and τ for convenience. To help explain the analysis that follows, the above state- space equation is written in a more compact form

$$\dot{\mathbf{x}}(t)=\mathbf{A}(t)\mathbf{x}(t)+\mathbf{B}(t)\mathbf{x}(t-\tau). \quad (24)$$

Equation (24) is now on the standard form of Eq. (4). Therefore, the state-space TFEA approach explained earlier can be used to construct a dynamic map similar to Eq. (14). However, in this case $\mathbf{\Phi}$ is no longer an identity matrix, instead, it is rather the state transition matrix

$$\mathbf{\Phi}=\frac{1}{\lambda_1-\lambda_2}\begin{bmatrix}\lambda_1 e^{\lambda_2 t_f}-\lambda_2 e^{\lambda_1 t_f} & e^{\lambda_1 t_f}-e^{\lambda_2 t_f}\\ \lambda_1\lambda_2 e^{\lambda_2 t_f}-\lambda_1\lambda_2 e^{\lambda_1 t_f} & \lambda_1 e^{\lambda_1 t_f}-\lambda_2 e^{\lambda_2 t_f}\end{bmatrix}, \quad (25)$$

where $\lambda_{1,2}=\zeta\pm\sqrt{\zeta^2-1}$, while t_f is the duration of free vibration. This state transition matrix relates the state of the tool as it exits the cut to its state as it re-enters the cut [1].

Some stability charts of Eq. (24) are shown in Fig. 6. The results obtained here with the state-space TFEA approach agree with the stability results in Ref. [23]. Perhaps the most interesting result is the appearance of closed islands of period doubling as shown in Fig. 6-b.

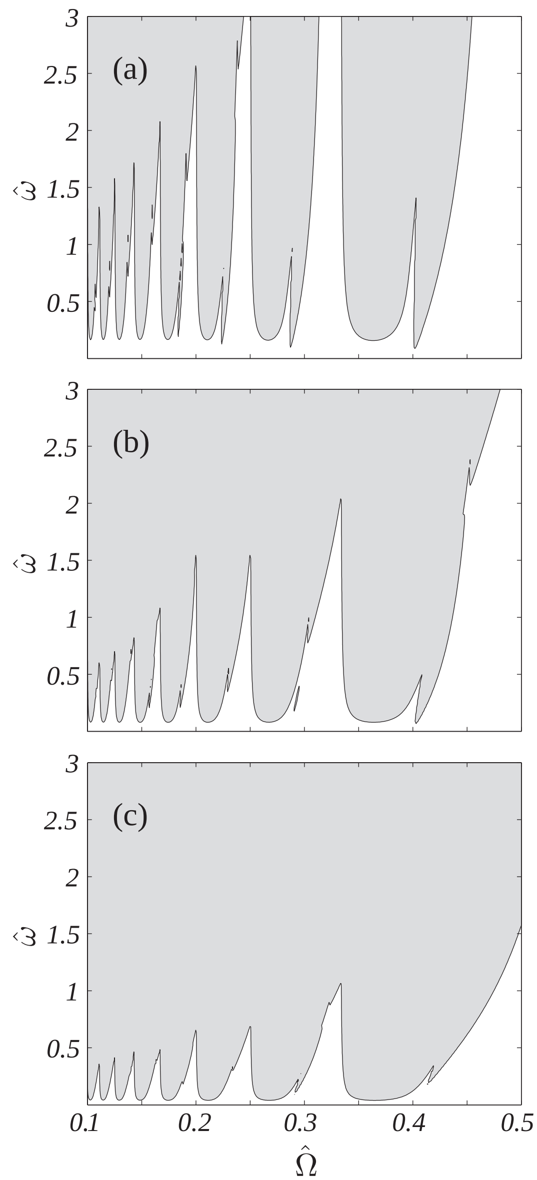

Figure 6. Stability diagrams of Eq. (22) for $\zeta=0.0038$ and (a) $\rho=0.05$, (b) $\rho=0.1$, and (c) $\rho=0.2$. Unstable regions are shaded while stable regions are left unshaded.

SUMMARY AND DISCUSSION

This paper presents a temporal finite element analysis approach for investigating the stability behavior of linear autonomous and nonautonomous DDEs. In contrast to the results of prior works on TFEA, which could only be applied to second order DDEs, the present work is applicable to a broader class of systems that may be written in the form of a state space model. The first section describes an introductory example, an

Copyright © 2009 by ASME

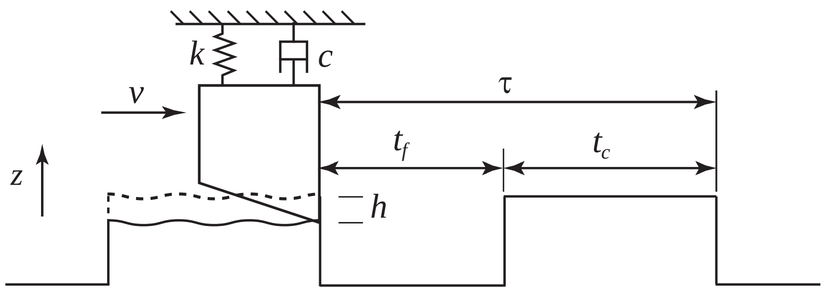

Figure 5. Schematic diagram of the interrupted cutting process. The force is proportional to the uncut chip area when the tool is in contact with the work piece but drops to zero when the tool vibrates freely [7].

autonomous DDE with a single state, prior to generalizing the formulation to linear DDEs with multiple states. The presented examples extend the described approach to time-periodic DDEs and piecewise continuous equations as was shown through an interrupted turning example.

An important consideration for the presented approach is the choice of trial and weighting functions. In particular, the illustration of Fig. 1 highlights the fact that the trial functions were chosen so that a single coefficient of the assumed solution would equal the state variable at the beginning, middle, and end of the temporal element. This provides three constraints for interpolating the polynomials with the remaining constraints being used to ensure orthogonality and meet user-preferences. During the course of this research, we have found Eq. (7a)-(7c) to be a particularly useful set of polynomials because higher order polynomials sometimes caused round-off errors for smaller temporal elements (i.e. seventh order polynomials would require that t_j^7 remain within the machine precision). Our choice of Legendre polynomials for weighting functions was based upon a few factors. First, we made comparisons with the weighting functions used in recent works (e.g. see reference [7]) and also implemented a Galerkin procedure. In both cases, we found that converged stability boundaries were obtained with fewer elements when using Legendre polynomials. However, we make no claim that the current set of trial and weighting functions are the most optimum set of polynomials. Another consideration is the number of weighting functions to apply. While our preference was to use a combination of two weighting functions and three trial functions, which will always keep the $\mathbf{G}$ and $\mathbf{H}$ matrices square, it is certainly possible to use more weighting functions.

Since the TFEA method is a discretization approach, a brief discussion of solution convergence seems necessary. Following the work in spatial finite elements, we recognize three different approaches for solution convergence: 1) the number of temporal elements can be increased (h-convergence); 2) the polynomial order may be increased (p-convergence); or 3) both the polynomial order and number of elements can be increased (hp-convergence). While a much more comprehensive discussion is offered in reference [25], it suffices to say that tracking the characteristic multipliers while increasing the number of elements or polynomial order may be used for convergence. For the present manuscript, we simply increased the number of temporal elements for each figure until a converged result was obtained.

In summary, the presented TFEA method provides a computationally efficient method to query the asymptotic stability of DDEs written in the form of a state space model. The method is useful for examining the stability of autonomous and non-autonomous DDEs with continuous as well as piece-wise continuous coefficients. A specific limitation of the presented work is that it is only applicable to DDEs that contain a single time delay. However, the extension of the presented approach to both nonlinear DDEs and DDEs with multiple time delays is a planned area of future research.

ACKNOWLEDGMENTS

Support from U.S National Science Foundation CAREER Award (CMMI-0757776) is gratefully acknowledged.

REFERENCES

[1] Mann, B. P., and Young, K. A., 2006. "An empirical approach for delayed oscillator stability and parametric identification". *Proceedings of the Royal Society A,* **462**, pp. 2145–2160.

[2] Balachandran, B., 2001. "Non-linear dynamics of milling process". *Proceedings of the Royal Society of London A,* **359**, pp. 793–819.

[3] Insperger, T., and Stépán, G., 2000. "Remote control of periodic robot motion". In Proceedings of 13th CISM-IFToMM Symposium on Theory and Practice of Robots and Manipulators, pp. 197–203.

[4] Batzel, J. J., and Tran, H. T., 2000. "Stability of the human respiratory control system. part i: Analysis of a two-

Copyright © 2009 by ASME

dimensional delay state-space model". *Journal of Mathematical Biology,* **41**, pp. 45–79.

[5] Stépán, G., 2001. "Modelling nonlinear regenerative effects in metal cutting". *Philosophical Transactions of the Royal Society of London A,* **359**, pp. 739–757.

[6] Olgac, N., and Sipahi, R., 2005. "A unique methodology for chatter stability mapping in simultaneous machining". *Journal of Manufacturing Science and Engineering,* **127**, pp. 791–800.

[7] Bayly, P. V., Halley, J. E., Mann, B. P., and Davis, M. A., 2003. "Stability of interrupted cutting by temporal finite element analysis". *Journal of Manufacturing Science and Engineering,* **125**, May, pp. 220–225.

[8] Insperger, T., Wahi, P., Colombo, A., Stépán, G., Bernardo, M., and Hogan, S. J., 2009. "Full characterization of act-and-wait control for first order unstable lag processes". *Journal of Vibration and Control*. In press.

[9] Liu, L., and Kalmár-Nagy, T., 2009. "High dimensional harmonic balance analysis for second-order delay-differential equations". *Journal of Vibration and Control*. In press.

[10] Stépán, G., 1989. *Retarded Dynamical Sytems: Stability and Characteristic Functions*. John Wiley & Sons.

[11] Hale, J. K., and Lunel, S. V., 1993. *Introduction to functional differential equations*. Springer-Verlag, New York.

[12] Insperger, T., and Stépán, G., 2002. "Stability chart of the delayed mathieu equation.". *Proceedings of Royal Society of London A,* **458**, pp. 1989–1998.

[13] Mann, B. P., Bayly, P. V., Davies, M. A., and Halley, J. E., 2004. "Limit cycles, bifurcations, and accuracy of the milling process". *Journal of Sound and Vibration,* **277**, pp. 31–48.

[14] Insperger, T., and Stépán, G., 2002. "Semi-discretization method for delayed systems". *International Journal for Numerical Methods in Engineering,* **55**(5), pp. 503–518.

[15] Fried, I., 1969. "Finite element analysis of time dependent phenomena". *AIAA Journal,* **7**, pp. 1170–1173.

[16] Argyris, J. H., and Scharpf, D. W., 1969. "Finite elements in time and space". *Aeronautical Journal of the Royal Society,* **73**, pp. 1041–1044.

[17] Borri, M., Bottasso, C., and Mantegazza, P., 1992. "Basic features of the time finite element approach for dynamics". *Meccanica,* **27**, pp. 119–130.

[18] Mann, B. P., Garg, N. K., Young, K. A., and Helvey, A. M., 2005. "Milling bifurcations from structural asymmetry and nonlinear regeneration". *Nonlinear Dynamics,* **42**, pp. 319–337.

[19] Mann, B. P., and Patel, B. R., 2009. "Stability of delay equations written as state space models". *Journal of vibration and control*. In press.

[20] Hayes, N. D., 1950. "Roots of the transcendental equations associated with certain differential-difference equations". *Journal of the London Mathematical Society,* **25**, pp. 226–232.

[21] Reddy, J. N., 1993. *An Introduction To The Finite Element Method*, 2 ed. McGraw-Hill, Inc., New York, NY.

[22] Kálmar-Nagy, T., 2005. "A new look at the stability analysis of delay differential equations". In Proceedings of International Design Engineering Technical Conferences and Computers and Information in Engineering Conference, Long Beach, California, DETC2005-84740, ASME.

[23] Szalai, R., and Stépán, G., 2006. "Lobes and lenses in the stability chart of interrupted turning". *Journal of Computational and Nonlinear Dynamics,* **1**, pp. 205–211.

[24] Szalai, R., and Stépán, G., 2006. "Lobes and lenses in the stability chart of interrupted turning". *Journal of Computational and Nonlinear Dynamics,* **1**, pp. 205–211.

[25] Garg, N. K., Mann, B. P., Kim, N. H., and Kurdi, M. H., 2007. "Stability of a time-delayed system with parametric excitation". *Journal of Dynamic Systems Measurement and Control,* **129**, pp. 125–135.

Copyright © 2009 by ASME